NeuroImage: Clinical 25 (2020) 102147

Contents lists available at ScienceDirect

NeuroImage: Clinical

journal homepage: www.elsevier.com/locate/ynicl

Electrophysiological resting state networks of predominantly akinetic-rigid Parkinson patients: Effects of dopamine therapy

Lukas Schneider[a], Valentin Seeger[a], Lars Timmermann[a,b], Esther Florin[a,c,*]

[a] Department of Neurology, University Hospital Cologne, Kerpener Strasse 62, 50937 Köln, Germany
[b] Department of Neurology, University Hospital Marburg, Baldingerstrasse, 35043 Marburg, Germany
[c] Institute of Clinical Neuroscience and Medical Psychology, Medical Faculty, Heinrich-Heine University Düsseldorf, Universitätsstr. 1, 40225 Düsseldorf, Germany

ARTICLE INFO

Keywords:
Dopamine
EEG
Resting state networks
Parkinson's disease

ABSTRACT

Parkinson's disease (PD) causes both motor and non-motor symptoms, which can partially be reversed by dopamine therapy. These symptoms as well as the effect of dopamine may be explained by distinct alterations in whole-brain architecture. We used functional connectivity (FC) and in particular resting state network (RSN) analysis to identify such whole-brain alterations in a frequency-specific manner. In addition, we hypothesized that standard dopaminergic medication would have a normalizing effect on these whole brain alterations. We recorded resting-state EEGs of 19 PD patients in the medical OFF and ON states, and of 12 healthy age-matched controls. The PD patients were either of akinetic-rigid or mixed subtype. We extracted RSNs with independent component analysis in the source space for five frequency bands. Within the sensorimotor network (SMN) the supplementary motor area (SMA) showed decreased FC in the OFF state compared to healthy controls. This finding was reversed after dopamine administration. Furthermore, in the OFF state no stable SMN beta component could be identified. The default mode network showed alterations due to PD independent of the medication state. The visual network was altered in the OFF state, and reinstated to a pattern similar to healthy controls by medication. In conclusion, PD causes distinct RSN alterations, which are partly reversed after levodopa administration. The changes within the SMN are of particular interest, because they broaden the pathophysiological understanding of PD. Our results identify the SMA as a central network hub affected in PD and a crucial effector of dopamine therapy.

1. Introduction

Understanding a complex disease like Parkinson's disease (PD) requires investigating whole-brain alterations. A promising recent approach is studying the brain at rest, i.e. without a specific task, because it offers insights into the large-scale functional organization of the whole brain. By now, it is well known that brain activity at rest separates into resting state networks (RSN). Because the RSN involve multiple brain structures with distinct functional roles, alterations visible in the RSN might potentially explain a variety of clinical features in PD. Motor symptoms in PD are commonly ascribed to pathological oscillations in beta and tremor-frequency ranges. At the same time, treatment of motor symptoms with levodopa is thought to restore such oscillations to a normal level. The relevance of oscillations makes a frequency-specific electrophysiological network approach a promising research avenue. The goal of the present study was therefore twofold: investigating frequency-specific pathological network alterations in PD and analyzing the effects of dopaminergic medication on these network alterations.

For PD pathological beta hypersynchronization has been identified within the subthalamic nucleus (STN) and between the STN and motor cortex of PD patients (Hirschmann et al., 2011, Hirschmann et al., 2013; Kühn et al., 2008; Neumann et al., 2017; Oswal et al., 2016; Tinkhauser et al., 2017; Weinberger et al., 2006). These beta oscillations were suppressed either by dopamine (Hirschmann et al., 2013; Neumann et al., 2017; Tinkhauser et al., 2017) or deep brain stimulation (DBS) (Abbasi et al., 2018; Kühn et al., 2008; Oswal et al., 2016), which are used as therapeutic means in PD. This suggests that beta oscillations are pathological. Based on these findings we hypothesized that in particular alterations in the beta frequency range are present in the motor-network and that those alterations are reduced through dopamine. In addition, the whole-brain resting state analysis of this study

* Corresponding author at: Institute of Clinical Neuroscience and Medical Psychology, Medical Faculty, Heinrich-Heine University Düsseldorf, Universitätstr. 1, 40225 Düsseldorf, Germany.
E-mail address: esther.florin@hhu.de (E. Florin).

https://doi.org/10.1016/j.nicl.2019.102147
Received 12 August 2019; Received in revised form 21 November 2019; Accepted 21 December 2019
Available online 10 January 2020

contrasting PD patients with healthy control subjects promises further valuable insight into altered brain networks and non-motor symptoms of PD.

To investigate non-motor symptoms, most previous studies have so far relied on functional magnetic resonance imaging (fMRI). Graph analysis on fMRI data revealed nodal and global efficiency decreases in PD patients compared to healthy controls (Skidmore et al., 2011) and distinct changes in the connectivity pattern in multiple brain regions of PD patients, involving both motor and non-motor regions (Skidmore et al., 2013). PD and drug-induced Parkinsonism exhibit a different resting state functional connectivity (FC) in fMRI, which hints at connectivity changes specific to PD, extending beyond the dopaminergic system (Ham et al., 2015). RSN alterations in PD patients were associated with deteriorating cognitive performance (Baggio et al., 2014, 2015). Newly diagnosed PD patients revealed alterations in multiple RSNs, including the sensorimotor, visual, and default mode network (Fang et al., 2017). fMRI, however, does not provide any frequency-specific information. Longitudinal graph-theoretic approaches with MEG also found a link between frequency-specific RSN alterations and deteriorating motor and cognitive performance (Olde Dubbelink et al., 2014a, 2014b). Therefore, in the present study, we aimed at extending these insights to frequency-specific RSN alterations. Since the most widely reported changes in fMRI RSN due to PD are within the sensorimotor, visual, and default mode network (de Schipper et al., 2018; Fang et al., 2017; Göttlich et al., 2013; Pelzer et al., 2019), we focused our analysis on these 3 networks. This choice is also advocated by the clinical symptoms, because PD often triggers cognitive deterioration and visual hallucinations besides classic motor symptoms.

The PD patients in most previous studies were either studied ON or OFF medication, preventing a direct investigation of medication effects. In a combined fMRI and PET approach dopamine levels modulated FC patterns in PD (Baik et al., 2014). Moreover, there is evidence from resting state analysis pointing towards a specific local effect of levodopa administration on the supplementary motor area (SMA), which was generally suppressed in PD (Casarotto et al., 2019; Esposito et al., 2013; Skidmore et al., 2013; Wu et al., 2009). Even though levedopa medication is still considered the standard therapy for PD, there remain substantial therapeutic limitations due to side effects resulting both in motor and non-motor symptoms (Fahn, 2015; You et al., 2018). Thus, a better understanding of levodopa effects on global brain properties is instrumental for improving pharmacologic therapy of PD in the future.

In the present study we recorded high-density EEG of patients ON and OFF medication as well as a healthy control group. From these data we extracted the resting state networks at the source level with an approach adapted from Brookes et al. (2011). This approach improves upon previous electrophysiological studies of PD by not confining the analysis to predefined regions of interest. This is particularly important as frequency-specific network alterations in PD are not yet sufficiently understood to define such regions of interest (ROI) with confidence. Moreover, defining seed regions always implies a certain amount of subjectivity. In contrast, our approach allows whole-brain network extraction without potentially confounding the data analysis by prior definition of an ROI. Using this approach, we aimed at identifying whole-brain network alterations in Parkinson's disease and the effect of standard dopaminergic medication. Based on the previous literature we expected i) alterations in the motor-network of Parkinson patients in the beta frequency range and ii) a mitigating effect of dopamine on those alterations. Furthermore, we hypothesized that dopamine generally restores RSN properties of PD patients to a more physiological pattern.

2. Materials and methods

2.1. Participants

We recruited 19 right-handed PD patients and 12 age- and handedness-matched, neurologically and psychiatrically healthy control participants (See Table 1). The experimental procedure was explained to all participants; they gave written consent afterwards. The study was approved by the local ethics committee (Cologne study nos. 14–129 and 14–264) and conducted in accordance with the Declaration of Helsinki. We assessed the Edinburgh Handedness Inventory for each participant to control for handedness. To exclude any cognitive impairments, all participants had to complete the Mini Mental Status Examination (MMSE). We assessed the Beck Depression Inventory II (BDI-II) for all subjects to exclude any depressive episode with the cut-off set at >20, “moderate depression” (Smarr and Keefer, 2011). To categorize PD subtypes, we evaluated the Unified Parkinson Disease Rating Scale III (UPDRS III) during off medication, and obtained a tremor score (sum of items 20–21 divided by 7 [total number of subitems]) and a non-tremor score (sum of items 18, 19, 22, 27–31 divided by 12 [total number of subitems]), similar to Spiegel et al. (2007). To classify a patient as akinetic-rigid a patient's non-tremor score had to be at least twice the tremor score. Otherwise patients were categorized as mixed type.

Table 1
Descriptive statistics of participants: UPDRS III = Unified Parkinson Disease Rating Scale, MMSE = Mini Mental Status Examination, BDI-II = Beck Depression Inventory-II.

Patients	
N	22
Females	5
Males	17
Complete exclusion from further analysis	3
Recorded ON state	17
Recorded OFF state	17
Age (mean ± SD)	65,1y ± 7,1y
Disease duration (mean ± SD)	7,6y ± 4,2y
Levodopa dose equivalent (mean ± SD)	242 mg ± 92 mg
UPDRS III (mean ± SD) ON	18 ± 8
UPDRS III (mean ± SD) OFF	30 ± 9
MMSE (mean ± SD)	28,4 ± 1,5
Edinburgh handedness test (mean ± SD)	81,5 ± 19,6
BDI-II (mean ± SD)	8,5 ± 5,4
Akinetic-rigid type	12
Mixed-type	7
Controls	
N	12
Females	1
Males	11
Age (mean ± SD)	65,1y ± 6,7y
MMSE (mean ± SD)	29 ± 0,8
Edinburgh handedness test (mean ± SD)	75,6 ± 26,9
BDI-II (mean ± SD)	4,8 ± 4,7

2.2. Data acquisition

All participants were told to sit relaxed in our EEG chamber and to fixate on a cross. EEG measurement was performed with a 128 EEG-channel actiCAP®, sampling rate at 2.5 kHz. The so-called “active electrodes” amplify the signal to increase the signal-to-noise ratio (SNR). We aimed at impedances < 25 kOhm. Eye movements and cardiac activity were recorded simultaneously with vertical electrooculography (EOG) and electrocardiography (ECG). Electrode positions were digitized using a Zebris® ultrasound device. During the actual EEG recordings, we made sure all subjects stayed awake by monitoring them with a camera system. We measured the control participants for 30 min each, split in 10 min blocks. To make sure PD patients were in clinical medication OFF, all PD medication had to be paused for at least 12 h prior to the EEG measurement. Before sitting in the scanner, an experienced motor disorder specialist assessed the individual UPDRS III motor score for each patient in the OFF state. We then recorded 10

continuous minutes of resting state EEG data. Afterwards patients were given the equivalent of their medical morning dose in form of rapidly-effective levodopa. To ensure a stable ON, we waited at least for 30 min, and then assessed the upper limbs UPDRS III sub-items. We then repeated 10 min of resting state EEG recording and afterwards assessed a second full UPDRS III score in the ON state. Additionally, we performed an individual coronar T1 MRI scan for each participant (3T Tim Trio Siemens, Erlangen, Germany, 1 × 1 × 1 mm voxel size, 5 patients with a voxel size of 0.48 × 0.48 × 2 mm).

2.3. Preprocessing

Noisy and flat EEG channels were excluded from further analysis. The data were then manually scanned in Brainstrom (http://neuroimage.usc.edu/brainstorm/Introduction, Version 27-Apr-2016) for noisy segments, which were also excluded. Segments recorded in states of drowsiness, according to the video recordings, were excluded, too. Eye blink and cardiac artifacts from the EOG and ECG recordings were then automatically removed via Signal-Space Projection (SSP). After pre-processing a mean data length for patients OFF medication of 463 ± 155 s; ON medication of 414 ± 140 s, and healthy controls 912 ± 227 s was obtained. The mean number of channels excluded per subject were for the patients OFF medication 15 ± 8, for the patients ON medication 15 ± 7, and for the healthy controls 28 ± 14.

Individual cortical surfaces (white matter – gray matter) were calculated from individual MRI scans using Freesurfer (http://freesurfer.net, v.5.3.0). Individual EEG sensor positions were imported to Brainstorm using the Zebris® data and matched to the head surfaces. EEG recordings were resampled to 1000 Hz. We then solved the forward problem with an OpenMEEG boundary element method (BEM), as implemented in Brainstorm (Gramfort et al., 2010; Kybic et al., 2005). For source reconstruction a diagonal noise covariance based on the complete resting state recording was calculated and the weighted minimum norm estimate (wMNE) was obtained for each subject.

2.4. Network extraction

The network extraction was based on the approach of Brookes et al. (2011): The source-reconstructed data were split into five frequency bands: δ (1–4 Hz), θ (4–8 Hz), α (8–13 Hz), β (13–30 Hz), and γ (30–50 Hz), and the Hilbert envelope for each band was calculated with Matlab. The envelope time-series were normalized using z-scoring, downsampled to 1 Hz, and spatially smoothed with a Gaussian Kernel of 5 mm full width at half maximum (FWHM) in Brainstorm. We then projected the envelope data onto the Colin27 anatomy (Holmes et al., 1998) using Freesurfer's registered spheres (visualization properties: amplitude threshold 0.3, minimum size 10 voxels), and z-scored the data.

To extract the network components based on the approach by Brookes et al. (2011), we performed a temporal Independent Component Analysis (ICA) at the group level and extracted 20 components for each frequency band (Calhoun et al., 2001). To extract stable components regardless of initial conditions for optimization, we used 50 resampling cycles and grouped the components in 20 estimated clusters as implemented in the ICASSO 1.22 toolbox (Himberg et al., 2004). Each cluster, i.e. network, was represented by a centrotype, which is the estimate that best represents all other estimates in the same cluster. By afterwards using the GroupICA approach, we also obtained maps for each participant (Calhoun et al., 2001). To obtain spatial resting state networks the temporal independent components (the centrotype from the ICASSO run) were correlated with the envelope data and these correlation maps were plotted. These correlation maps for each of the analyzed frequency bands were compared to standard fMRI RSN. We defined RSNs based on the fMRI 17-network parcellation of the human cerebral cortex (Yeo et al., 2011), and computed the spatial overlap D between the EEG resting state networks, which were thresholded for correlation values below 0.3, and the fMRI-based resting state maps (Mesmoudi et al., 2013):

$$D(EEG_{RSN}, RSN_{fMRI-based}) = \frac{EEG_{RSN} \cap RSN_{fMRI-based}}{EEG_{RSN} \cup RSN_{fMRI-based}}$$

The overlap is calculated for each voxel or cortical source. If there is a perfect spatial overlap between an EEG RSN and one fMRI map, D will be 1. We thereby obtained the best fitting EEG RSN for each group (healthy controls, patients ON, patients OFF).

2.5. Network comparison

To identify significant differences between the spatial extent of specific network components, we performed independent t-tests across subjects for each source between the best fitting components for each resting state network in each frequency band (ON versus OFF, controls versus ON, controls versus OFF). An independent *t*-test was also used for the comparison between the medication states, because not all patients had a good EEG recording both with and without medication. After Bonferroni correction for number of vertices where we use 0.001 as the significance threshold, we also control for 28 conditions (patients OFF vs. ON vs. controls, and 5 frequency bands) to obtain a significance threshold of $p < 0.028 = 28 * 0.001$.

2.5.1. Data availability

Because of privacy law, data are available upon personal request. Enquiries can be sent to the corresponding author.

3. Results

3.1. Sociodemographic and clinical features

The study involved 22 patients with idiopathic Parkinson's disease (PD). Two patients were completely left out from further analysis due to large movement artifacts. For two patients each the ON and OFF medication recording, respectively, were excluded due to artifacts. One patient had a BDI-II score above 20 and was therefore excluded. In total, 17 OFF and 17 ON datasets from 19 right-handed patients were included (5 females, 14 males, aged 65.1 ± 7.1 years, mean ± SD; Edinburgh handedness score 81.5 ± 19.6, mean ± SD; disease duration of 7.6 ± 4.2, mean ± SD). 7 of those PD patients were of mixed-type (7 OFF and 7 ON recordings) and 12 of akinetic-rigid (10 OFF and 10 ON recordings) subtype according to the classification of Spiegel et al. (2007). No tremor-dominant patients were included. After the OFF measurement patients were administered 242 mg ± 92 mg Levodopa (mean ± SD), improving the UPDRS III from 30 ± 9 (off score, mean ± SD) to 18 ± 8 (on score, mean ± SD). MMSE testing revealed no cognitive impairment (28.4 ± 1.5, mean ± SD).

We also included 12 right-handed healthy age-matched controls (age 65.1 ± 6.7 years, mean ± SD; Edinburgh handedness score 75.6 ± 26.9, mean ± SD, 1 female). None of the control participants was diagnosed with any neurological or psychiatric disorder, nor showed any form of cognitive impairment (MMSE 29.0 ± 0.8, mean ± SD) or depressive symptoms (BDI-II 4.8 ± 4.7, mean ± SD).

3.2. Network components

After preprocessing the EEG data we extracted resting state networks with the approach from Brookes et al. (2011) for the Parkinson patients and the healthy controls. In the following we will focus on the sensorimotor, visual, and default mode network.

3.2.1. Sensorimotor network

The common fMRI sensorimotor network (SMN) consists of bilateral primary motor and somatosensory regions and the supplementary

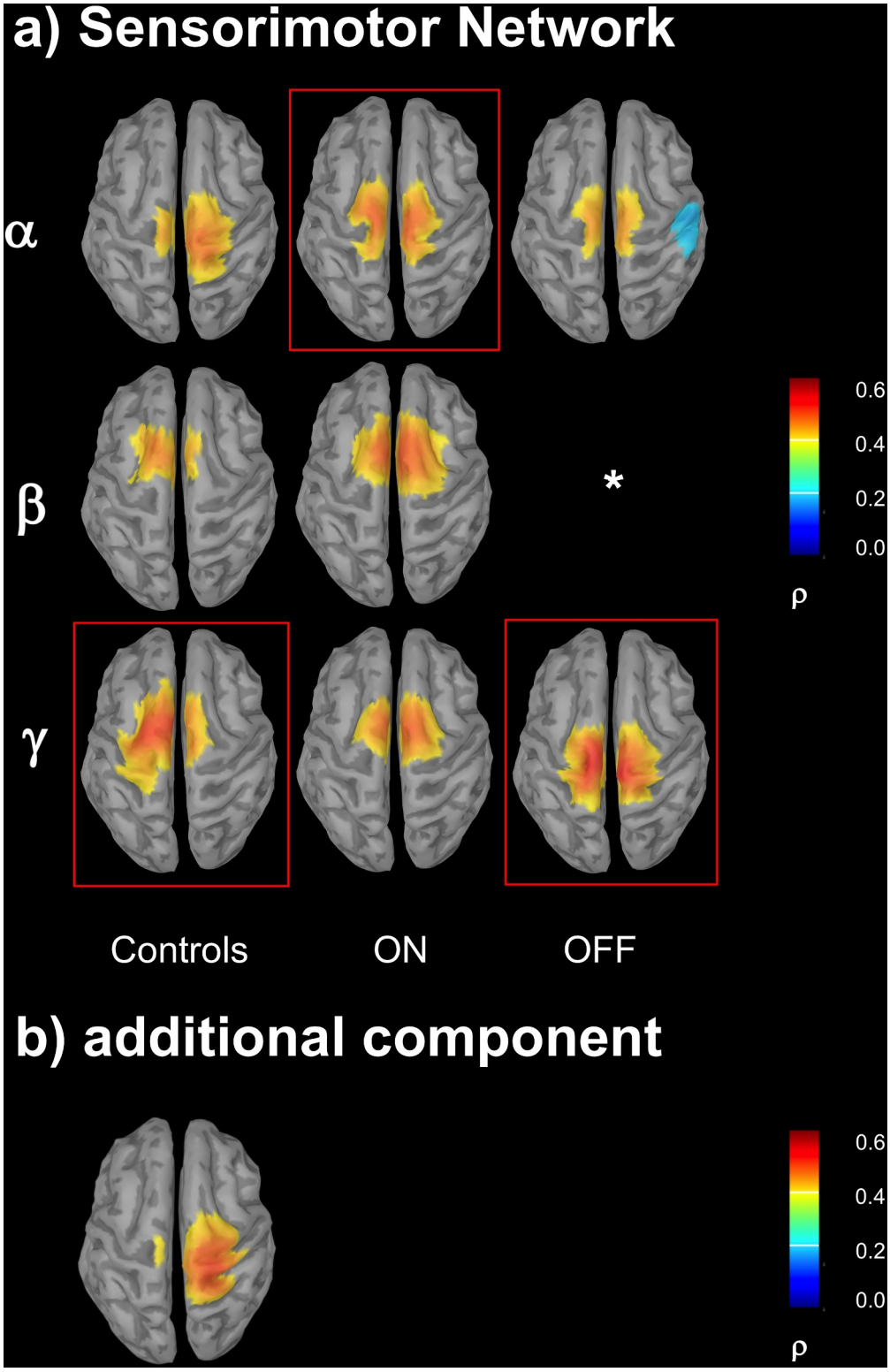

Fig. 1. Sensorimotor EEG Network. a) Sensorimotor Network: bestfitting components highlighted in red (controls – gamma, ON – alpha, OFF – gamma). *no stable beta component could be extracted from patients OFF medication. The values plotted correspond to the correlation value between IC component and the envelope time-series. (For interpretation of the references to color in this figure legend, the reader is referred to the web version of this article.)

motor area (SMA). ICA components for the SMN were found in the alpha, beta, and gamma band (see Fig. 1a). Interestingly, in the OFF medication state no beta IC component representing the SMN could be identified.

Both for healthy controls and patients OFF medication the gamma component was spatially best-fitting (see Table 2 and Fig. 1a). Of note, the SMN of the healthy control group was split into a left and a right hemispheric part (Fig. 1b). The SMN of patients ON medication was found best-fitting in the alpha band. When comparing the best-fitting components, the SMN showed a peri- and post-central increase for both ON and OFF medication versus healthy controls (see Table 3). No significant differences were found between patients ON and OFF

Table 2
Sensorimotor network, visual and default mode network: components best-fitting to the fMRI based RSN for each group. A theoretical coefficient D = 1 would imply perfectly identical network properties.

	Sensorimotor network	Visual network	Default mode network
Controls	gamma (D = 0.37)	delta (D = 0.49)	theta (D = 0.13)
OFF	gamma (D = 0.42)	alpha (D = 0.49)	beta (D = 0.25)
ON	alpha (D = 0.41)	delta (D = 0.4)	Beta (D = 0.23)

medication. Subgrouping revealed no significant differences between akinetic-rigid and mixed-type patients.

Comparison of the SMN within each frequency band revealed significant differences within the beta and gamma band (see Table 3). Patients OFF medication showed a significant decrease in the SMA and an increase within the posterior regions of the SMN in gamma frequencies compared to healthy controls and patients ON medication (Fig. 2a). These gamma alterations compared to healthy controls were reversed ON medication. In the beta band we only found a minor significant increase in the right interhemispheric fissure in patients ON medication versus controls (Fig. 2b). There was no stable beta band SMN for patients OFF medication.

3.2.2. Visual network

The visual network consists of the primary and secondary visual cortices in the occipital lobes. It was spatially best matched to the fMRI based RSN in delta (control group and patients ON medication) and alpha frequencies (patients OFF medication) (see Table 2 and Fig. 3a).

3.2.3. Default mode network

The Default Mode Network (DMN) was split into a bifrontal medial component and two components covering the inferior parietal cortex. No stable posterior cingulate cortex (PCC) component was extracted. We therefore focused on the bifrontal component, because frontal areas are particularly modulated by dopamine (Kahnt and Tobler, 2017; Nieuwenhuys et al., 2008). The component best-fitting to the fMRI-based RSN for the healthy control group was found in the theta band (Fig. 3b), while components from the patient groups both ON and OFF medication were best-fitted in the beta range.

4. Discussion

This present work is to our knowledge the first study to investigate EEG whole-brain cortical resting state alterations of Parkinson patients by contrasting them with a healthy control group. To this end, we adapted a data-driven approach from Brookes et al. (2011) to the use with EEG data. With this approach we were able to identify whole brain networks without the inherent subjectivity or potential bias due to defining regions of interest prior to network extraction. Importantly, within the healthy control group we were able to extract stable resting state networks as known from the fMRI literature. For unmedicated PD patients the FC within the SMN to the SMA was suppressed in the gamma band. This effect was reversed after levodopa administration. These findings extend our pathophysiological understanding of PD, especially in terms of an altered motor network structure and its reinstatement after dopamine intake.

4.1. EEG resting state networks in healthy elderly subjects

For the control subjects we could extract stable components from various frequency bands for well-established resting state networks, including the SMN, the DMN, and the visual network. These networks were spatially matched with networks described in the fMRI literature. This confirms that the resting state analysis works for EEG data. The SMN of the elderly healthy controls was found in alpha, beta, and gamma frequencies, which is in line with previous findings (Nugent et al., 2017; Sockeel et al., 2016). Best spatially matched was the gamma component. The main SMN component did not span both hemispheres equally, but was split into two components (see Fig. 1b). Previously, the SMN has been reported to be dominated by beta oscillations (Brookes et al., 2011; Mantini et al., 2007). However, these studies investigated the RSNs of younger healthy subjects. To our knowledge the only study investigating older healthy participants (mean age 72 years) reports both beta and gamma frequencies for the SMN (Hillebrand et al., 2012). Another group scanned participants aged 18 to 87 years with EEG and reports a spatial cross-frequency organization of the SMN with beta and gamma components (Aoki et al., 2015). Even though the aforementioned electrophysiological studies investigated heterogeneous age groups, they provide evidence that healthy aging might contribute to network reorganization and thus also frequency alterations, in particular in motor networks.

Supporting evidence of this conjecture comes from fMRI results that convincingly indicate that aging specifically affects the sensorimotor network. For example, a complex pattern of FC increases and decreases with aging affecting cortical and cerebellar motor networks has been described by Seidler et al., 2015. Another fMRI study reported increased FC from the sensorimotor cortex of healthy elderly and reduced FC from the mid-posterior insula. Moreover, age could be predicted by this reduced FC, strongly indicating a physiological re-organization of the SMN with aging (He et al., 2016). In contrast, electrophysiological findings on aging effects are more challenging to interpret. Asymmetrical spectral power alterations were reported from the motor cortex, with increased beta and gamma band activity in both hemispheres (Cottone et al., 2013). Brain networks of healthy adults increase in size with aging in beta and gamma frequencies (Schlee et al., 2012). This is another hint at alterations especially in beta and gamma frequencies and suggest that further research on electrophysiological correlates of healthy aging might be fruitful.

4.2. Patients

The SMN in the gamma frequency range of the unmedicated patients exhibited a significant decrease in frontal areas, including the SMA, whereas it was enlarged in posterior regions when compared with healthy controls and patients ON medication ($p < 0.001$). There were no significant spatial differences between healthy controls and patients ON medication for the SMA. Our results therefore provide evidence for an impaired SMN for PD patients at rest, particularly in the SMA at gamma frequencies, which is reinstated after levodopa treatment.

Electrophysiological findings on medication effects within the SMA

Table 3
Sensorimotor network: Independent t-tests for significant inter-group differences of best-fitting components and within frequency bands ($p < 0.028$). *no stable SMN component for patients OFF medication, therefore no comparison to controls and patients ON medication possible.

	Inter-group comparison	Beta band	Gamma band
ON vs. OFF	No significant differences	-*	OFF: SMA decreased, increased posterior network properties
Controls vs. ON	ON: increased posterior properties	no significant differences	spatial network properties very similar, only minor increase in the right interhemispheric fissure
Controls vs. OFF	OFF: increased posterior properties, decreased SMA	-*	OFF: SMA decreased, increased posterior network properties

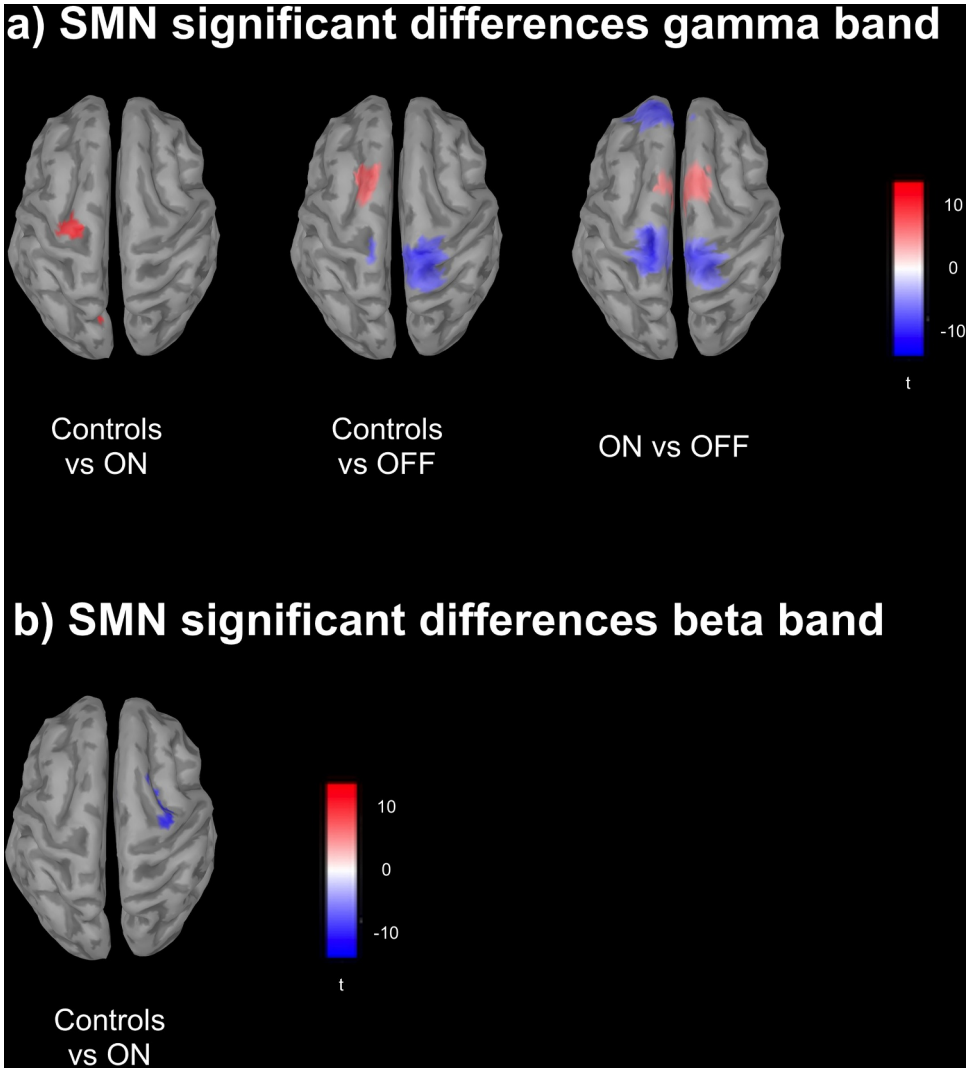

Fig. 2. Sensorimotor EEG Network group differences. a) Significant group differences in the gamma band: Medication OFF shows a reduced SMN in frontal areas, in particular Brodmann area 6, containing the SMA, compared to both healthy controls and medication ON. On the other hand, the SMN is enhanced bilaterally in peri- and postcentral regions. Remarkably, there are only modest differences for the SMA in ON vs healthy controls ($p < 0.028$). b) Significant group differences in the beta band: Controls vs ON in beta; note only minor significant differences in right hemispheric precentral regions ($p < 0.028$).

are rare. One study reported an over-activation for the SMA of PD patients versus healthy controls at gamma frequencies (Moazami-Goudarzi et al., 2008). However, this study combined patients with and without levodopa intake, which somewhat complicates insights into possible levodopa effects. Nonetheless, it hints at a crucial role of gamma oscillations within the SMA of PD patients. Moreover, PD patients have altered motor loops including the SMA, both during internally and externally paced repetitive finger movements (Herz et al., 2014a, Herz et al., 2014). Levodopa was shown to reinstate more physiological connectivity patterns in these loops, particularly in high beta and gamma frequencies. Recently, levodopa intake was shown to reduce beta-band desynchronization in the SMA during a motor task, further pointing to a pivotal role of the SMA in pathological network organization in PD patients and as a possible effector of levodopa treatment (Chung et al., 2018).

The effects of levodopa treatment have been investigated in more detail with fMRI: The first fMRI study to investigate FC within the motor network of PD patients found decreases in the SMA for patients OFF medication and normalizations after 250 mg levodopa intake. Importantly, all patients received a standard dosage, rather than dosages based on their individual anti-Parkinsonian medication (Wu et al., 2009). These findings are in line with another fMRI study, investigating the amplitude of low frequency fluctuations (ALFF) as a marker of brain activity during rest (Skidmore et al., 2013). ALFF signals in the SMA were lower in patients OFF medication than in healthy controls. Suppressed FC within the SMA was reported when comparing controls and untreated PD patients (Esposito et al., 2013). Furthermore, levodopa increased FC especially in the SMA of PD patients both versus healthy controls and a placebo group. Recently it has been shown with transcranial magnetic stimulation (TMS) and EEG that levodopa intake increases the excitability nearby the SMA (Casarotto et al., 2019). These results likewise suggest a disengagement especially of the SMA in PD that is reversed by levodopa administration, possibly through locally restoring a more physiological network mechanism.

Taken together, our study provides further evidence for the hypothesis that the SMA is a central hub for the patho-mechanism of PD and for levodopa effects at rest.

4.3. SMN in the beta range

Interestingly, we did not find a beta SMN component for the patients OFF medication, suggesting a disrupted network architecture of the whole SMN, particularly in beta frequencies. In contrast, after levodopa administration, we found a stable SMN component in the beta

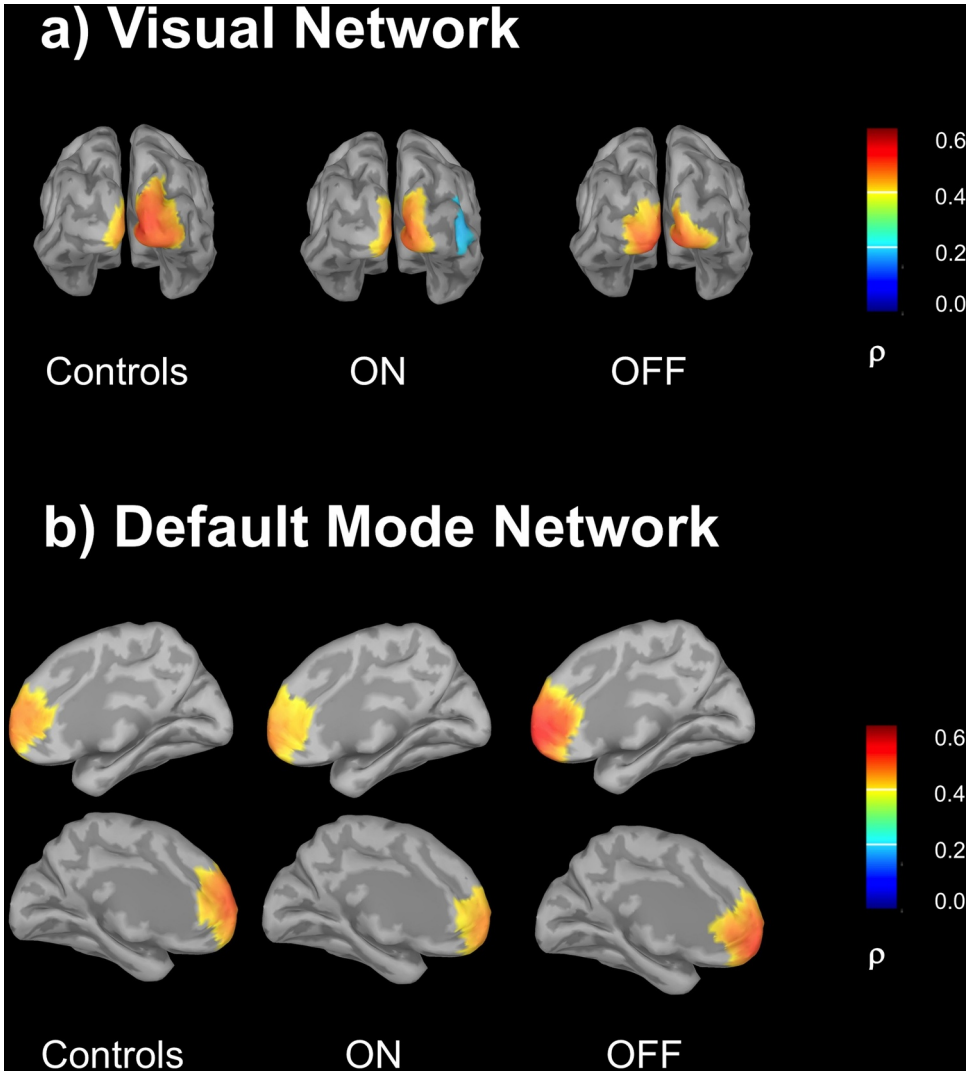

Fig. 3. Visual and Default Mode EEG Networks, bestfitting components. a) Visual Network: controls – delta, ON – delta, OFF – alpha. b) Default Mode Network: controls – theta, ON – beta, OFF – beta. Note that we concentrated on the bifrontal parts, because these are known to be particularly modulated by dopamine. The values plotted correspond to the correlation value between IC component and the envelope time-series.

band of PD patients. Moreover, there were only minor significant differences between controls and PD patients ON medication in the beta band. Our findings therefore suggest that the SMN is suppressed in the OFF state, notably in beta frequencies. Levodopa seemingly restores the SMN to a spatial pattern almost identical to healthy controls, and effectively improves motor function.

Beta oscillations have been identified to play an essential role within the motor cortex. They aid post-movement motor inhibition in healthy controls and are desynchronized during movement (Heinrichs-Graham et al., 2017). Furthermore, the SMN from healthy subjects is dominated by beta oscillations (Hillebrand et al., 2012; Mantini et al., 2007). Therefore, one might speculate that an impaired SMN at beta frequencies crucially contributes to motor symptoms of PD patients.

A potential explanation might be based on pathological beta hypersynchronization within the Subthalamic Nucleus (STN) and between the STN and motor cortices, which has been reported by numerous studies (Hirschmann et al., 2011, Hirschmann et al., 2013; Kühn et al., 2008; Neumann et al., 2017; Tinkhauser et al., 2017; Weinberger et al., 2006). At first glance a state of hyper-synchronization seems to imply increased resting state connectivity and thus potentially a stronger beta component for the SMN. This would contradict our results. But there is evidence from a MEG study reconciling these two conflicting findings. Beta oscillations of PD patients OFF medication were actually decreased during rest in the motor cortex compared to healthy controls (Heinrichs-Graham et al., 2014). Furthermore, they were restored after dopamine administration, thus a normalizing effect was hypothesized which is in line with our results. Interestingly, the aforementioned study also reported a beta hypersynchrony between left and right motor cortices in the unmedicated patients, which was reduced after levodopa administration. This finding might provide a connecting link between pathological beta-hypersynchrony on the one hand, and reduced FC within motor areas during resting state on the other hand.

Selection bias might pose another challenge at interpreting the previous literature on pathological beta oscillations from PD. The electrophysiological activity of the STN is only detectable through deep brain stimulation (DBS) electrodes. The reported pathological findings from the STN usually are from severely affected patients with a long disease duration. The patients in our study had an average disease duration of 7 years and had no DBS electrodes implanted, making a direct linking to the STN activity infeasible. Such a direct comparison linking resting state activity from deep-brain structures and cortical networks would require a whole-brain investigation.

4.4. Default mode network

The DMN was seemingly split into the bifrontal medial cortex and

left and right inferior parietal cortex components. We concentrated on the bifrontal components (Kahnt and Tobler, 2017; Nieuwenhuys et al., 2008). For the healthy elderly it was found in theta frequencies. This contrasts with previous MEG findings which extracted it from alpha frequencies (Brookes et al., 2011). Interestingly, this study did not find a PCC component, either. They speculated that due to the relatively low spatial resolution of MEG for deeper brain regions they did not identify the PCC. The same logic should apply to our EEG results. Another study found the DMN best correlated to alpha and beta oscillations (Mantini et al., 2007). However, when participants were instructed to alternate between self-referencing and concentrating on breathing the DMN was determined in the theta band (Fomina et al., 2015). Simultaneous electrocorticographic and fMRI recordings from epilepsy patients revealed a spatial correspondence for the DMN in the theta band (Hacker et al., 2017). Taken together, these findings suggest a widely distributed frequency pattern for the DMN.

Interestingly, we found the DMN in the beta band for patients both ON and OFF medication. This suggests an effect on the DMN that goes beyond the effects of pure dopamine depletion. Akinetic-rigid PD patients have a disrupted DMN architecture even in a state of normal cognitive function and gray matter volume (Hou et al., 2017). Our patient cohort consisted of akinetic-rigid and mixed-type patients without cognitive deficits. Thus, our findings in the DMN are in line with the fore-cited study. The akinetic-rigid subtype in particular is associated with faster cognitive decline compared to tremor-dominant patients (Thenganatt and Jankovic, 2014). Alterations in the DMN structure might therefore provide a valuable link to cognitive deterioration, even in early sub-clinical stages.

4.5. Visual network

We found the best-fitting components for the visual network of the healthy elderly within the delta band. Within the OFF medication group, it was located in the alpha band, whereas it changed back to the delta band ON medication. These findings suggest an altered frequency pattern in the visual network in PD, as well as a normalizing effect of levodopa.

Our findings are in line with previous work reporting a wide range of alterations in visual networks from fMRI data. Newly diagnosed PD patients with medication history of less than a week revealed disruptions in visual networks using graph theoretical analysis (Fang et al., 2017). Studying PD patients with and without visual hallucinations revealed a reduced FC in the occipital lobe for both groups versus healthy controls (Hepp et al., 2017). De Schipper et al. (2018) studied both standard fMRI RSNs and eigenvector centrality mapping (EC) in PD patients. Contrary to the aforementioned study an increased FC in occipital regions within the PD patient group was described. Contrastingly, EC was reduced. Göttlich et al., 2013 report decreased interaction of the visual network with other brain areas for PD patients. This suggests that changes in the visual network are part of a broader pattern of brain alterations in PD.

4.6. Methodological considerations

Finally, we would like to highlight three methodological considerations of our study.

First, our patient cohort consisted of akinetic-rigid and mixed-type PD subtypes with advanced disease stages. No tremor-dominant patients as classified by their UPDRS sub-scores based on Spiegel et al. (2007) were included. Different PD subtypes have been shown to exhibit different metabolic and longitudinal characteristics (Eggers et al., 2011, 2012, 2014). Therefore, one should be careful when applying our findings to PD patients in general.

Second, EEG has a high temporal resolution, but somewhat lacks spatial resolution. However, RSNs span large portions of the brain. Therefore, the lack of spatial resolution does not result in major implications for the extraction of robust networks. By solving the inverse problem prior to further analysis, we could extract the RSNs based on the cortical map. This considerably improves the interpretability of our results.

Third, the choice of the number of ICs is always slightly arbitrary. Brookes et al. (2011) used 25 ICs for MEG data. However, for our EEG data with its lower number of channels it was not possible to obtain 25 stable ICs for all frequency bands. Therefore, we reduced the number of ICs to 20. These 20 ICs still allowed us to extract the 3 networks that we investigated in detail in the present study.

5. Conclusion

The present study was designed to identify electrophysiological RSN alterations due to PD within distinct frequency bands. We hypothesized dopamine would reinstate the network structure of PD patients, possibly through providing an alternative rather than an identical network composition. Indeed, the SMN for the PD patients OFF medication is affected at rest, particularly through a reduced FC of the SMA at gamma frequencies. This effect is reversed after levodopa intake. These findings emphasize the role of the SMA both as a central network hub in the pathophysiology of PD and a potential target of levodopa treatment. Additionally, the SMN in the beta band is missing in the OFF medication state and is reinstated after levodopa intake. This further highlights the importance of beta band alterations in PD within integral parts of the motor network. We therefore suggest that the reintegration of motor networks in the beta band is connected to the clinical motor improvements after levodopa treatment. Changes in DMN were found somewhat independently from levodopa. This could be related to early cognitive decline. Taken together, in the present study alterations in the RSN architecture provided insights into pathophysiologic processes which might be involved in distinct clinical features of PD. This link to clinical symptoms is worth further exploration.

CRediT authorship contribution statement

Lukas Schneider: Visualization, Project administration, Methodology, Formal analysis, Data curation, Writing - original draft. **Valentin Seeger:** Formal analysis, Data curation, Writing - review & editing. **Lars Timmermann:** Formal analysis, Writing - review & editing. **Esther Florin:** Visualization, Project administration, Formal analysis, Writing - review & editing.

Acknowledgments

This work was supported by the German Research Foundation [Clinical Research Group 219]. EF gratefully acknowledges support by the Volkswagen Foundation (Lichtenberg program 89387).

References

Abbasi, O., Hirschmann, J., Storzer, L., Ozkurt, T.E., Elben, S., Vesper, J., Wojtecki, L., Schmitz, G., Schnitzler, A., Butz, M., 2018. Unilateral deep brain stimulation suppresses alpha and beta oscillations in sensorimotor cortices. NeuroImage 174, 201–207.

Aoki, Y., Ishii, R., Pascual-Marqui, R.D., Canuet, L., Ikeda, S., Hata, M., Imajo, K., Matsuzaki, H., Musha, T., Asada, T., Iwase, M., Takeda, M., 2015. Detection of EEG-resting state independent networks by eLORETA-ICA method. Front. Hum. Neurosci. 9, 31.

Baggio, H.C., Sala-Llonch, R., Segura, B., Marti, M.J., Valldeoriola, F., Compta, Y., Tolosa, E., Junque, C., 2014. Functional brain networks and cognitive deficits in Parkinson's disease. Hum. Brain Mapp. 35, 4620–4634.

Baggio, H.C., Segura, B., Sala-Llonch, R., Marti, M.J., Valldeoriola, F., Compta, Y., Tolosa, E., Junque, C., 2015. Cognitive impairment and resting-state network connectivity in Parkinson's disease. Hum. Brain Mapp. 36, 199–212.

Baik, K., Cha, J., Ham, J.H., Baek, G.M., Sunwoo, M.K., Hong, J.Y., Shin, N.Y., Kim, J.S., Lee, J.M., Lee, S.K., Sohn, Y.H., Lee, P.H., 2014. Dopaminergic modulation of resting-state functional connectivity in de novo patients with Parkinson's disease. Hum. Brain Mapp. 35, 5431–5441.

Brookes, M.J., Woolrich, M., Luckhoo, H., Price, D., Hale, J.R., Stephenson, M.C., Barnes, G.R., Smith, S.M., Morris, P.G., 2011. Investigating the electrophysiological basis of resting state networks using magnetoencephalography. Proc. Natl. Acad. Sci. USA 108, 16783–16788.

Calhoun, V.D., Adali, T., Pearlson, G.D., Pekar, J.J., 2001. A method for making group inferences from functional MRI data using independent component analysis. Hum. Brain Mapp. 14, 140–151.
Casarotto, S., Turco, F., Comanducci, A., Perretti, A., Marotta, G., Pezzoli, G., Rosanova, M., Isaias, I.U., 2019. Excitability of the supplementary motor area in Parkinson's disease depends on subcortical damage. Brain Stimul. 12, 152–160.
Chung, J.W., Burciu, R.G., Ofori, E., Coombes, S.A., Christou, E.A., Okun, M.S., Hess, C.W., Vaillancourt, D.E., 2018. Beta-band oscillations in the supplementary motor cortex are modulated by levodopa and associated with functional activity in the basal ganglia. Neuroimage Clin. 19, 559–571.
Cottone, C., Tomasevic, L., Porcaro, C., Filligoi, G., Tecchio, F., 2013. Physiological aging impacts the hemispheric balances of resting state primary somatosensory activities. Brain Topogr. 26, 186–199.
de Schipper, L.J., Hafkemeijer, A., van der Grond, J., Marinus, J., Henselmans, J.M.L., van Hilten, J.J., 2018. Altered whole-brain and network-based functional connectivity in Parkinson's disease. Front. Neurol. 9, 419.
Eggers, C., Kahraman, D., Fink, G.R., Schmidt, M., Timmermann, L., 2011. Akinetic-rigid and tremor-dominant Parkinson's disease patients show different patterns of FP-CIT single photon emission computed tomography. Mov. Disord. 26, 416–423.
Eggers, C., Pedrosa, D.J., Kahraman, D., Maier, F., Lewis, C.J., Fink, G.R., Schmidt, M., Timmermann, L., 2012. Parkinson subtypes progress differently in clinical course and imaging pattern. PLoS One 7, e46813.
Eggers, C., Schwartz, F., Pedrosa, D.J., Kracht, L., Timmermann, L., 2014. Parkinson's disease subtypes show a specific link between dopaminergic and glucose metabolism in the striatum. PLoS One 9, e96629.
Esposito, F., Tessitore, A., Giordano, A., De Micco, R., Paccone, A., Conforti, R., Pignataro, G., Annunziato, L., Tedeschi, G., 2013. Rhythm-specific modulation of the sensorimotor network in drug-naive patients with Parkinson's disease by levodopa. Brain 136, 710–725.
Fahn, S., 2015. The medical treatment of Parkinson disease from James Parkinson to George Cotzias. Mov. Disord. 30, 4–18.
Fang, J., Chen, H., Cao, Z., Jiang, Y., Ma, L., Ma, H., Feng, T., 2017. Impaired brain network architecture in newly diagnosed Parkinson's disease based on graph theoretical analysis. Neurosci. Lett. 657, 151–158.
Fomina, T., Hohmann, M., Scholkopf, B., Grosse-Wentrup, M., 2015. Identification of the default mode network with electroencephalography. Conf. Proc. IEEE Eng. Med. Biol. Soc. 2015, 7566–7569.
Göttlich, M., Münte, T.F., Heldmann, M., Kasten, M., Hagenah, J., Kramer, U.M., 2013. Altered resting state brain networks in Parkinson's disease. PLoS One 8, e77336.
Gramfort, A., Papadopoulo, T., Olivi, E., Clerc, M., 2010. OpenMEEG: opensource software for quasistatic bioelectromagnetics. Biomed. Eng. Online 9, 45.
Hacker, C.D., Snyder, A.Z., Pahwa, M., Corbetta, M., Leuthardt, E.C., 2017. Frequency-specific electrophysiologic correlates of resting state fMRI networks. NeuroImage 149, 446–457.
Ham, J.H., Cha, J., Lee, J.J., Baek, G.M., Sunwoo, M.K., Hong, J.Y., Shin, N.Y., Sohn, Y.H., Lee, J.M., Lee, P.H., 2015. Nigrostriatal dopamine-independent resting-state functional networks in Parkinson's disease. NeuroImage 119, 296–304.
He, H., Luo, C., Chang, X., Shan, Y., Cao, W., Gong, J., Klugah-Brown, B., Bobes, M.A., Biswal, B., Yao, D., 2016. The functional integration in the sensory-motor system predicts aging in healthy older adults. Front. Aging Neurosci. 8, 306.
Heinrichs-Graham, E., Kurz, M.J., Becker, K.M., Santamaria, P.M., Gendelman, H.E., Wilson, T.W., 2014. Hypersynchrony despite pathologically reduced beta oscillations in patients with Parkinson's disease: a pharmaco-magnetoencephalography study. J. Neurophysiol. 112, 1739–1747.
Heinrichs-Graham, E., Kurz, M.J., Gehringer, J.E., Wilson, T.W., 2017. The functional role of post-movement beta oscillations in motor termination. Brain Struct. Funct. 222, 3075–3086.
Hepp, D.H., Foncke, E.M.J., Olde Dubbelink, K.T.E., van de Berg, W.D.J., Berendse, H.W., Schoonheim, M.M., 2017. Loss of functional connectivity in patients with Parkinson disease and visual hallucinations. Radiology 285, 896–903.
Herz, D.M., Florin, E., Christensen, M.S., Reck, C., Barbe, M.T., Tscheuschler, M.K., Tittgemeyer, M., Siebner, H.R., Timmermann, L., 2014a. Dopamine replacement modulates oscillatory coupling between premotor and motor cortical areas in Parkinson's disease. Cereb. Cortex 24, 2873–2883.
Herz, D.M., Siebner, H.R., Hulme, O.J., Florin, E., Christensen, M.S., Timmermann, L., 2014. Levodopa reinstates connectivity from prefrontal to premotor cortex during externally paced movement in Parkinson's disease. NeuroImage 90, 15–23.
Hillebrand, A., Barnes, G.R., Bosboom, J.L., Berendse, H.W., Stam, C.J., 2012. Frequency-dependent functional connectivity within resting-state networks: an atlas-based MEG beamformer solution. NeuroImage 59, 3909–3921.
Himberg, J., Hyvärinen, A., Esposito, F., 2004. Validating the independent components of neuroimaging time series via clustering and visualization. NeuroImage 22, 1214–1222.
Hirschmann, J., Ozkurt, T.E., Butz, M., Homburger, M., Elben, S., Hartmann, C.J., Vesper, J., Wojtecki, L., Schnitzler, A., 2011. Distinct oscillatory STN-cortical loops revealed by simultaneous MEG and local field potential recordings in patients with Parkinson's disease. NeuroImage 55, 1159–1168.
Hirschmann, J., Ozkurt, T.E., Butz, M., Homburger, M., Elben, S., Hartmann, C.J., Vesper, J., Wojtecki, L., Schnitzler, A., 2013. Differential modulation of STN-cortical and cortico-muscular coherence by movement and levodopa in Parkinson's disease. NeuroImage 68, 203–213.
Holmes, C.J., H.R., Collins L, Woods, R., Toga, A.W., Evans, A.C., 1998. Enhancement of MR images using registration for signal averaging. J. Comput. Assist. Tomogr. 22 (2), 324–333.
Hou, Y., Luo, C., Yang, J., Ou, R., Liu, W., Song, W., Gong, Q., Shang, H., 2017. Default-mode network connectivity in cognitively unimpaired drug-naive patients with rigidity-dominant Parkinson's disease. J. Neurol. 264, 152–160.
Kahnt, T., Tobler, P.N., 2017. Dopamine modulates the functional organization of the orbitofrontal cortex. J. Neurosci. 37, 1493–1504.
Kühn, A.A., Kempf, F., Brucke, C., Gaynor Doyle, L., Martinez-Torres, I., Pogosyan, A., Trottenberg, T., Kupsch, A., Schneider, G.H., Hariz, M.I., Vandenberghe, W., Nuttin, B., Brown, P., 2008. High-frequency stimulation of the subthalamic nucleus suppresses oscillatory beta activity in patients with Parkinson's disease in parallel with improvement in motor performance. J. Neurosci. 28, 6165–6173.
Kybic, J., Clerc, M., Abboud, T., Faugeras, O., Keriven, R., Papadopoulo, T., 2005. A common formalism for the integral formulations of the forward EEG problem. IEEE Trans. Med. Imaging 24, 12–28.
Mantini, D., Perrucci, M.G., Del Gratta, C., Romani, G.L., Corbetta, M., 2007. Electrophysiological signatures of resting state networks in the human brain. Proc. Natl. Acad. Sci. USA 104, 13170–13175.
Mesmoudi, S., Perlbarg, V., Rudrauf, D., Messe, A., Pinsard, B., Hasboun, D., Cioli, C., Marrelec, G., Toro, R., Benali, H., Burnod, Y., 2013. Resting state networks' corticotopy: the dual intertwined rings architecture. PLoS One 8, e67444.
Moazami-Goudarzi, M., Sarnthein, J., Michels, L., Moukhtieva, R., Jeanmonod, D., 2008. Enhanced frontal low and high frequency power and synchronization in the resting EEG of Parkinsonian patients. NeuroImage 41, 985–997.
Neumann, W.J., Staub-Bartelt, F., Horn, A., Schanda, J., Schneider, G.H., Brown, P., Kuhn, A.A., 2017. Long term correlation of subthalamic beta band activity with motor impairment in patients with Parkinson's disease. Clin. Neurophysiol. 128, 2286–2291.
Nieuwenhuys, R.V., Voogd, J., Van Huijzen, C., 2008. The Human Central Nervous System, 4 ed. Steinkopff-Verlag, Heidelberg.
Nugent, A.C., Luber, B., Carver, F.W., Robinson, S.E., Coppola, R., Zarate, C.A., 2017. Deriving frequency-dependent spatial patterns in MEG-derived resting state sensorimotor network: a novel multiband ICA technique. Hum. Brain Mapp. 38, 779–791.
Olde Dubbelink, K.T, Hillebrand, A., Stoffers, D., Deijen, J.B., Twisk, J.W., Stam, C.J., Berendse, H.W., 2014a. Disrupted brain network topology in Parkinson's disease: a longitudinal magnetoencephalography study. Brain 137, 197–207.
Olde Dubbelink, K.T, Schoonheim, M.M., Deijen, J.B., Twisk, J.W., Barkhof, F., Berendse, H.W., 2014b. Functional connectivity and cognitive decline over 3 years in Parkinson disease. Neurology 83, 2046–2053.
Oswal, A., Beudel, M., Zrinzo, L., Limousin, P., Hariz, M., Foltynie, T., Litvak, V., Brown, P., 2016. Deep brain stimulation modulates synchrony within spatially and spectrally distinct resting state networks in Parkinson's disease. Brain 139, 1482–1496.
Pelzer, E.A., Florin, E., Schnitzler, A., 2019. Quantitative susceptibility mapping and resting state network analyses in Parkinsonian phenotypes-a systematic review of the literature. Front. Neural Circuits 13, 50.
Schlee, W., Leirer, V., Kolassa, S., Thurm, F., Elbert, T., Kolassa, I.T., 2012. Development of large-scale functional networks over the lifespan. Neurobiol. Aging 33, 2411–2421.
Seidler, R., Erdeniz, B., Koppelmans, V., Hirsiger, S., Mérillat, S., Jäncke, L., 2015. Associations between age, motor function, and resting state sensorimotor network connectivity in healthy older adults. NeuroImage 108, 47–59.
Skidmore, F., Korenkevych, D., Liu, Y., He, G., Bullmore, E., Pardalos, P.M., 2011. Connectivity brain networks based on wavelet correlation analysis in parkinson fMRI data. Neurosci. Lett. 499, 47–51.
Skidmore, F.M., Yang, M., Baxter, L., von Deneen, K.M., Collingwood, J., He, G., White, K., Korenkevych, D., Savenkov, A., Heilman, K.M., Gold, M., Liu, Y., 2013. Reliability analysis of the resting state can sensitively and specifically identify the presence of Parkinson disease. NeuroImage 75, 249–261.
Smarr, K.L., Keefer, A.L., 2011. Measures of depression and depressive symptoms: beck depression inventory-ii (BDI-II), center for epidemiologic studies depression scale (CES-D), geriatric depression scale (GDS), hospital anxiety and depression scale (HADS), and patient health questionnaire-9 (PHQ-9). Arthritis Care Res. (Hoboken) 63 (Suppl 11), S454–S466.
Sockeel, S., Schwartz, D., Pelegrini-Issac, M., Benali, H., 2016. Large-scale functional networks identified from resting-state EEG using spatial ICA. PLoS One 11, e0146845.
Spiegel, J., Hellwig, D., Samnick, S., Jost, W., Mollers, M.O., Fassbender, K., Kirsch, C.M., Dillmann, U., 2007. Striatal FP-CIT uptake differs in the subtypes of early Parkinson's disease. J. Neural Transm. (Vienna) 114, 331–335.
Thenganatt, M.A., Jankovic, J., 2014. Parkinson disease subtypes. JAMA Neurol. 71, 499–504.
Tinkhauser, G., Pogosyan, A., Tan, H., Herz, D.M., Kuhn, A.A., Brown, P., 2017. Beta burst dynamics in Parkinson's disease off and on dopaminergic medication. Brain 140, 2968–2981.
Weinberger, M., Mahant, N., Hutchison, W.D., Lozano, A.M., Moro, E., Hodaie, M., Lang, A.E., Dostrovsky, J.O., 2006. Beta oscillatory activity in the subthalamic nucleus and its relation to dopaminergic response in Parkinson's disease. J. Neurophysiol. 96, 3248–3256.
Wu, T., Wang, L., Chen, Y., Zhao, C., Li, K., Chan, P., 2009. Changes of functional connectivity of the motor network in the resting state in Parkinson's disease. Neurosci. Lett. 460, 6–10.
Yeo, B.T., Krienen, F.M., Sepulcre, J., Sabuncu, M.R., Lashkari, D., Hollinshead, M., Roffman, J.L., Smoller, J.W., Zöllei, L., Polimeni, J.R., Fischl, B., Liu, H., Buckner, R.L., 2011. The organization of the human cerebral cortex estimated by intrinsic functional connectivity. J. Neurophysiol. 106, 1125–1165.
You, H., Mariani, L.L., Mangone, G., Le Febvre de Nailly, D., Charbonnier-Beaupel, F., Corvol, J.C., 2018. Molecular basis of dopamine replacement therapy and its side effects in Parkinson's disease. Cell Tissue Res. 373, 111–135.